Closed Loop Controlled Precision Irrigation Sensor Network

Levente J. Klein, Hendrik F. Hamann, *Member, IEEE*, Nigel Hinds, Supratik Guha, Luis Sanchez, Brent Sams, and Nick Dokoozlian

***Abstract*—A closed loop irrigation system is demonstrated that fully automates the delivery of irrigation and calculates the water requirement from satellite images. The system optimizes water delivery for 140 cells located across four hectares of land based on two independent objectives (e.g., maximizing yield and increasing water efficiency) and is continuously adapting irrigation scheduling to the local spatial–temporal variability of the vegetation across the growing season. Irrigation is controlled by a central computer that issues commands to 693 control nodes to start irrigation based on the analysis of satellite images. The control nodes are laid out to create 15 m × 15 m cells and each cell can be addressed independently and can irrigate differentially. After two years of operation, this variable rate drip irrigation approach resulted in a 26% yield increase in the second year and an average increase of 16% in water use efficiency. This paper demonstrates that combining closed loop automation and advanced irrigation analytics can improve the water use efficiency and increase the yield on existing agricultural lands.**

***Index Terms*—Automation, closed control loop, device-to-device communication, information processing, Internet, sensor network.**

I. Introduction

DIGITIZATION of the physical world is fundamentally changing the industries fueled by sensor networks, automation, and robotization [1]. Sensor-based decision support or automated infrastructure control can minimize manual intervention. In agriculture, data driven decisions can enable a sustainable use of water, land utilization, and chemicals control through optimized analytics [2].

Platforms that fuse sensor network data with automatic control can lead to dynamic operation that adapts to the environment in real-time as new data becomes available to the system. One important application in agriculture is irrigation, which can be controlled by sensor networks and automate the operation of the water delivery systems. Despite continuous advancement in control systems, irrigation is mostly a manual process using traditional practices.

Many of the high value crops in California, such as grapes, are drip irrigated with water usually applied uniformly across larger parcels or blocks of land. This often results in nonoptimized delivery of water, fertilizers, and pesticides. For example, intrafield soil water holding capacity can fluctuate significantly, often translating into as much as fivefold yield differences across less than a few meter distance [3].

To overcome such variability, management zones can be defined, where each zone may have similar yield or vigor characteristics (for grapes) and can be managed accordingly. Minimizing yield variability [4] through differential management [5] has been proposed in the past. Variable rate management in vineyards has been proposed both in USA [6] and in Australia [7] but only relying on post-harvest analysis. Management zones have been delineated based on soil [8], vegetation index [9], or using fuzzy logic clustering techniques [10]. While defining management zones is a well-established technique, active control of variable rate management is still not fully developed.

In the past, sensor networks have been deployed in vineyard settings [11] at various levels of sophistication. Most of the application attempted a better monitoring of the micro environmental conditions in the vineyards thereby providing a more granular feedback to vineyard workers [12].

Here, we present a large-scale demonstration of a variable rate drip irrigation system that takes advantage of a close loop control system to deliver the right amount of water through an automated system. Using this new variable drip irrigation technology, the applied water amount can be optimized dynamically. Ultimately, it is envisioned that such a system can be designed to deliver the optimum amount of water to each plant. Delivery of water to each management zone requires timely analytics to determine irrigation requirements, to transmit the irrigation schedule to a control computer, and to automate control of the drip irrigation infrastructure to dispense the optimum amount of water. In this paper, we show that a variable rate automatic irrigation system coupled with satellite derived irrigation scheduling analytics can result in: 1) increased yield uniformity and 2) reversal of the yield trends by increasing the yield on the originally low yield areas and limiting the yield on the originally high yield areas.

The advantage of a variable rate irrigation system is the increased yield on existing farm land without the need to convert additional land to agricultural use. The efficient use of

Manuscript received December 18, 2017; revised July 23, 2018; accepted July 25, 2018. Date of publication August 14, 2018; date of current version January 16, 2019. This work was internally funded by IBM and E. & J. Gallo. *(Corresponding author: Levente J. Klein.)*

L. J. Klein, H. F. Hamann, and N. Hinds are with the Internet of Things and Cognitive Industry Solutions, IBM T. J. Watson Research Center, Yorktown Heights, NY 10598 USA (e-mail: kleinl@us.ibm.com; nhinds@us.ibm.co).

S. Guha is with the Institute for Molecular Engineering, University of Chicago, Chicago, IL 60637 USA, and also with the Nanoscience and Technology Division, Argonne National Laboratory, Lemont, IL 60439 USA.

L. Sanchez, B. Sams, and N. Dokoozlian are with the E. & J. Gallo Winery, Modesto, CA 95353 USA.

Digital Object Identifier 10.1109/JIOT.2018.2865527

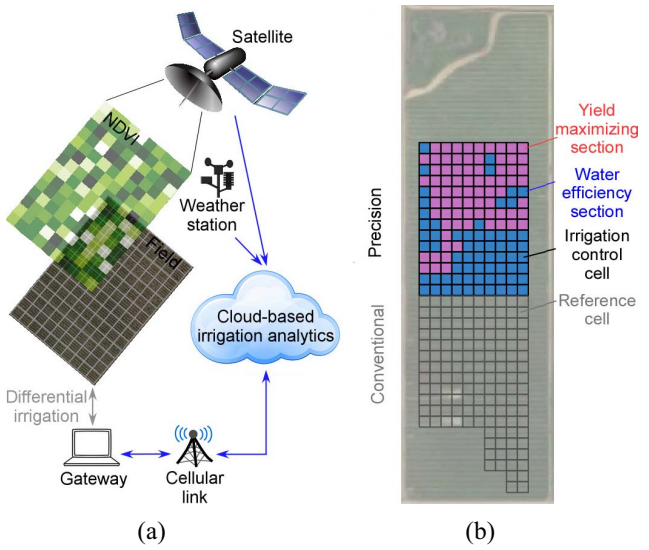

Fig. 1. (a) Schematic architecture of the closed control loop irrigation system driven by satellite imagery. (b) Precision irrigation area composed of water efficiency and yield maximizing sections.

technology not only can increase the yield on existing farm land but also promises to manage more efficiently resources like water and fertilizer. To the best of our knowledge, this paper constitutes the first and largest closed loop drip irrigation system that directly couples remote observations with an automated dense sensor network that is operated from the cloud. Not only the drip irrigation in our approach is fully automated but at the same time this system results in significant water savings while improving yield.

II. Sensor Network

A. System Architecture

The experiment is conducted on a 20-year-old, 12.4 hectare, drip irrigated Cabernet Sauvignon vineyard near Galt, CA, USA. A four hectare section of the vineyard containing the full range of yields, as reported by the 2012 yield map, is selected for the closed loop irrigation system. The irrigation system is changed from a single drip line to a double drip-line variable irrigation system with centrally controlled irrigation sensor network. The control system allows differential irrigation along segments of 15 m. A 15 m $\times$ 15 m area defined as "the irrigation control cell" is the basic unit of control where the water delivery within that area can be independently controlled (Fig. 1). The experimental area, called "Precision," is composed of 140 of such independent cells where cells are grouped in two sections "Yield maximizing section" and "Water efficiency section." These two differently managed sections have different objective functions: 1) maximize the yield and 2) increase water use efficiency. The area is monitored using satellite imagery that constitutes the input for irrigation requirement analytics. Besides monitoring the area, the closed loop system runs the analytics to determine the irrigation water requirement and controls the irrigation infrastructure to dispense the water. The analytics output is transmitted to a sensor network that dispense the water accordingly. The irrigation schedule is sent weekly to the irrigation system, where the

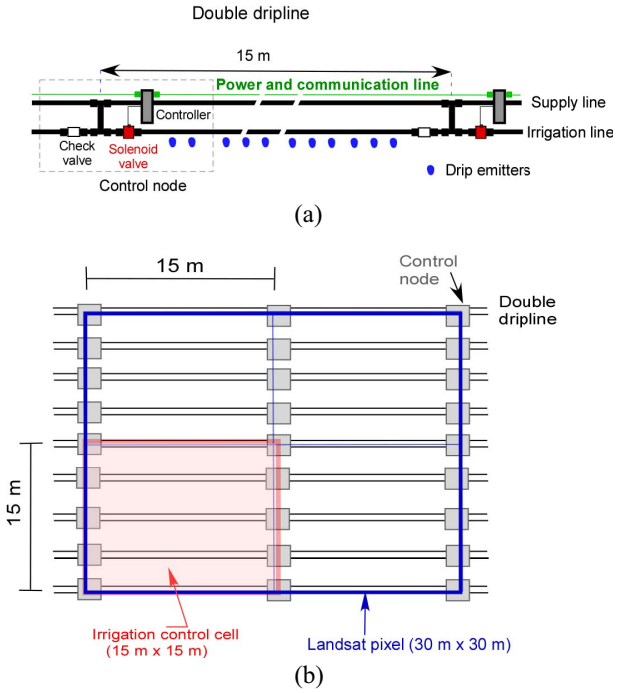

Fig. 2. (a) Double drip line composed of supply and irrigation lines connected through the control nodes that operate the solenoid valve. (b) Details of an irrigation control cell that groups 5 double drip lines and its spatial alignment with a Landsat satellite image pixel.

computer splits the schedule for 6 or 7 days irrigation and issues commands to the management zones. The outcome of the differential irrigation is monitored by the next satellite imagery that will indicate if expected change occurred and the irrigation water schedule is readjusted based on the new satellite images. An adjacent area, called "Conventional" area, having similar yield characteristics and soil composition as the Precision area in 2012, is uniformly irrigated to serve as a reference area. The closed loop irrigation system is automatically operated with minimal human input. We note that domain expertise related to adjustment in grape sugar content is required to be added to the irrigation schedule calculations. Additional data layers like high resolution drone or thermal images of the vineyard can be added to the analytics for monitoring canopy stresses that may not be detectable from satellite images.

B. Variable Rate Irrigation Infrastructure

For the variable rate infrastructure, the original single drip irrigation line is divided into a double drip line system consisting of a water supply line and an irrigation line and segmented into 15 m sections [Fig. 2(a)]. The supply line is always filled with water and is connected to the main water supply. The irrigation line can be filled once the solenoid valve is opened and the water is allowed to flow into that segment. The irrigation line has emitters installed that will let water drip and irrigate the soil. The supply and irrigation line are connected at each 15 m through a control node that allows water to be diverted from the supply line to the irrigation line. The control nodes consist of a solenoid valve, a controller, and a check valve. The controller issues the command to open/close the solenoid valve

Fig. 3. Photograph of the interior and controller box that operated the solenoid valve and the installed sensor network in the vineyard.

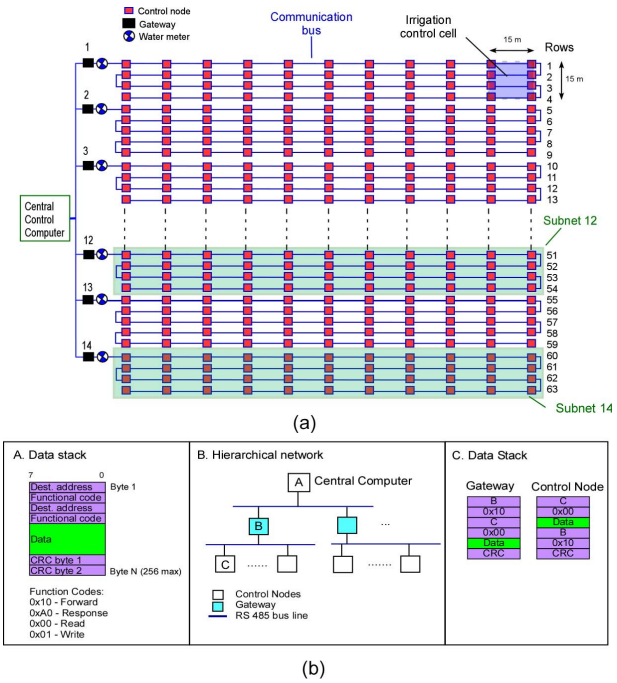

Fig. 4. (a) Schematics of the communication network between the central computer and control nodes composed of 14 subnets and 140 irrigation control cells. (b) Data communication stack and communication protocols between the central computer and control nodes.

and allows water to flow into the segment, while the check valve impedes water to fill the previous management segment. There is a power and communication line that runs along the supply line and connects each control node to a central control point. The controller nodes are installed at the edge of an area that establishes a one-to-one correspondence between the information extracted from a parcel of land (via satellite imagery and/or ground-based sensors) and a management area. We chose a 15 m $\times$ 15 m control cell dimension, higher than the original Landsat [13] pixel resolution (30 m $\times$ 30 m), which was used in this paper. The original 30 m $\times$ 30 m Landsat pixels are interpolated to 15 m $\times$ 15 m pixel size using pan sharpening and aligned exactly with the experimental 15 m $\times$ 15 m cells [Fig. 2(b)]. We note that managing vineyard at higher resolution than the satellite images did not provide any benefit as discussed in Section IV, as there is an optimal size for the control cells.

The control nodes are 15 m apart along each irrigation line segment (covering 10 vines) and the irrigation lines (and vine rows) are 3.3 m apart. Alternating, 4 or 5 control nodes are therefore lumped together to define each "irrigation control cell," which covers on average an area of 15 m $\times$ 15 m [Fig. 2(a)]. Since the vine rows could not be perfectly aligned with satellite pixel resolution, the number of rows entering in a cell is varied between 4 and 5 to create the digital footprint of satellite images on the irrigation system [Fig. 2(b)]. There are a total of 140 independent control cells, with 40 or 50 vines in each of the cells distributed across the four hectare area with a total of 693 control nodes (Fig. 3).

The irrigation schedule is managed by a central computer that issues the command to the local microcontroller that operates the solenoid valves to keep it open for the required amount of time. The amount of irrigation water dispensed is controlled by the time interval the solenoid valve is kept open and water drips through the drip emitters mounted on the irrigation line. Time synchronization between the local microcontroller and the central computer is carried out once per day.

In addition to actuating (open/close) the solenoid valve, each node keeps track of the time the valve is open and reports back to the control computer which aggregates the data and runs background calculations to verify that the system operates as expected.

C. Sensor Communication

The experimental area is divided in 14 subnets where each subnet contains 4 or 5 rows of grape rows. Along each subnet there are ten irrigation control cells. Each subnet is controlled by a gateway that receives and transmits the data from the central computer to the 40 or 50 control nodes [Fig. 4(a)] within that subnet. The central computer is distributing the irrigation schedule to the gateways and each gateway sends commands to individual control nodes under its command. The schematic of the message stack protocol for communicating is shown in Fig. 4(b). A command message is encapsulated in a queue stack. Each header contained a destination node address and a function code; the address field is 8 bits, the function code is 8 bits, and the check-sum is a 16 bit cyclic redundancy check (CRC) (see Fig. 4(b)-A). A specific example is shown in Fig. 4(b)-B, where the central computer communicates with a selected control node via a selected gateway. There are three required steps to get the message from the central computer to a selected control node and an additional three steps to send back an acknowledgment from the control node to the central computer. First, the central computer sends the message to a selected gateway. Second, the gateway, based on a "forwarding" function code, moves the first fixed length header to the trailer space in the

message and transmits the new message (Fig. 4(b)-C) simultaneously to all nodes in the subnet. The node for which the message is intended will recognize its unique address in the message. Once the control node performs the requested operation (e.g., open valve), it rewrites the data section leaving the header and trailer intact. As the central computer expects a response, the control node prepares the stack to be sent back. The control node transmits the response message to the gateway. The gateway processes the message by moving the first trailer (before the CRC) to the header and transmits the new message to the central computer. The central computer, expecting a response, processes the result and acknowledges that the message is successfully delivered to the control node. The transmitted command can be the irrigation requirements (number of minutes that the irrigation line needs to be filled with water) or just open/close commands at the beginning and end of the day to bring all control nodes into the same state. Each subnet includes a flow meter that measures the water consumption for the whole subnet. In each subnet there are 40 or 50 control boxes that are connected by serial bus communication wires to each gateway. At the end of the rows, wires that crossed rows, are buried underground. The communication line did not exceeds 1500 m as this value is tested to constitute the upper limit for signal integrity using RS485 communications. Irrigation of the 140 control cells is enabled by daily continuous communication with all 693 control nodes, where each node is uniquely identified (addressed) by a source routing technique that specifies a specific gateway-node pair.

A cellular link connects the central computer to the cloud-based analytics, allowing downloading irrigation schedules and remote diagnostics. A message notification system is implemented that alerts valve's malfunctioning or nonintended water usage.

The power lines extend to all control nodes and is fanned out at the start of each row. The power distribution system is optimized to maintain 12 V along each line such that controllers located farthest from the gateway can open/close the solenoid valves under normal operating conditions. While the current implementation is based on wired control, a wireless communication method had been prototyped and tested as a next generation system. For the wireless option, the power harvesting from solar panels required for operation could not be achieved due to the dense canopy and panel placement limitations dictated by daily maintenance work on the farm.

D. Irrigation Requirement Analytics

Landsat 7 and Landsat 8 imagery obtained from the U.S. Geological Survey [14] provides reflectance data in eight different spectral bands every 16 days (alternating by 8 days for each satellite). The vineyard investigated in this paper is on the overlapping section of path 43 row 34 and path 44 row 33 for Landsat 7 and 8, respectively, which provides a satellite observation every eight days.

Two of these spectral bands, the red (0.64–0.67 micrometer) and the near infrared (0.77–0.90 micrometer) are sensitive to vineyard canopy development [15] and are used to determine the NDVI [16]

$$\mathrm{NDVI} = \frac{\mathrm{NIR} - \mathrm{RED}}{\mathrm{NIR} + \mathrm{RED}} \tag{1}$$

where RED and NIR are the red and near infrared intensity values for each pixel in the image. The NDVI value varies between 0 and 1. Its value changes as the canopy develops through the growing season and its spatial distribution across a vineyard reflects the variability in vigor and ultimately the water holding capacity of the soil. All satellite images are corrected for atmosphere induced scattering [17].

The amount of water delivered to each cell is then calculated from the NDVI and the water loss due to evapo-transpiration (ET_0) using the Penman–Monteith equation [18]. The daily weather inputs (insolation, wind, temperature, and relative humidity) are obtained from the nearest California Irrigation Management Information System weather station (Fair Oaks, CA, USA) [19] to calculate the reference evapo-transpiration (ET_0).

The amount of water that is scheduled for irrigation ET_{cb} (in mm day^{-1}) is then calculated from the reference evapo-transpiration (ET_0) [20] and adjusted for grapes using the basal crop coefficient (k_{cb}) which serves as an aggregated coefficient of the physical and physiological characteristics of the plant [20]. A management factor, f, is included that can adjust the water delivered to each of the irrigation control cell

$$\mathrm{ET}_{cb} = f \cdot k_{cb} \cdot \mathrm{ET}_0. \tag{2}$$

The basal crop coefficient, k_{cb}, is calculated from the Mapping Evapo-Transpiration at High Resolution with Internalized Calibration model [21], [22] using the NDVI value for each cell. The basal crop coefficient can be obtained by subtracting the soil heat flux and sensible heat flux from the net radiation at the surface [22]. In case the Landsat data is obscured by clouds, the NDVI values are extrapolated using historical reflectance data from the same plot of the vineyard.

The irrigation schedule for each cell is based on (2), with the value of management factor, f, varied from 0.5 for the first eight weeks of irrigation up to 0.75 during the rest of the season in 2013. In 2014, the management factor, f, is 0.5 for the first five weeks and then increased to 0.7 for the rest of the season. The management factor, f, is used to apply moderate water stress to the vines and improve fruit quality and to increase yield in low vigor area. The management factor is a parameter that can be changed and it can incorporate domain knowledge or management practices on the farm.

The evapo-transpiration is calculated for the following week based on real-time weather data. The irrigation schedule for individual control cells is calculated using the NDVI value and ET_{cb} taking into account the number of drippers for each zone and dripper specifications (i.e., 1.89 l h^{-1}). Irrigation schedules are generated on a weekly basis for each zone and transmitted to the central control computer. Once a schedule is uploaded to the computer, it reads the zone number and number of hours per day that needs to enable the irrigation and issue a command to the control node containing the solenoid valve to open and allow water in the irrigation

line for the required time interval. Once the required irrigation time passes, the central computer issue a command to close the solenoid valve.

E. Variable Rate Management Zone Delineation

Based on the 2012 yield map, irrigation control cells that had a yield value below 20 tonnes hectare^{-1} and low NDVI value are grouped in two management zones: 1) the yield maximizing zones and 2) the water efficiency zones. The yield maximizing zones has low yield in 2012 and water is used to increase in that zone. The water efficiency area is targeted to minimize the water consumption. We note that there could be other objectives that can be implemented; e.g., reduce NDVI variability, reduce variability in grape quality, or minimize fertilizer use.

Many objectives can be tied to delineate zones based on spectral indices like NDVI that is readily available even for farm where historical yield or soil data may not exist.

F. Yield Analysis Methods

Crop yield maps are used to establish grape production variability [23], [24]. Crop yield maps are measured in 2012, 2013, and 2014 using the Advanced Technology Viticulture (ATV, Joslin, SA, Australia) yield monitor systems installed on three self-propelled, over-the-row, trunk-shaking mechanical GH9000 AIM harvesters (Ag Industrial Manufacturing, Lodi, CA, USA). The yield monitors included a differential global positioning system, a grape weighing unit and a data recording system. The grape weighing unit contains a load cell weight bridge and a belt speed sensor. Geo-referencing is realized by simultaneously logging the coordinates and synchronizing them with the weight measurements. The data is transferred to a computer and accessed using proprietary software from ATV. Belt scales are zeroed before each harvest and the system is calibrated against actual truck weights at the beginning of the harvest season and weekly thereafter.

Calibration is validated by ensuring that weight error ranges are within 8% of the weight at the winery, but actual measurements are consistently within 3%–4%. Harvest data is transferred into a data processing module developed in R Studio (RStudio Inc., Boston, MA, USA) to convert mass flow units into tonnes hectare^{-1}, to eliminate measurement points that are outliers, and to normalize measurements from different harvesters. Yield data with values larger than three standard deviations from the mean are removed. The data cleaning steps eliminates only 5% of the original data. After yield data cleaning, the data is further processed by a software package (VESPER Version 1.62) [25] for interpolation and kriging to 3 $\times$ 3 m resolution. The raster data sets are then transferred into a program (Manifold System, Manifold Net Ltd., Carson City, NV, USA), where a 3 m $\times$ 3 m geo-referenced grid is created. For this paper, the yield data is further aggregated to 15 m $\times$ 15 m geo-referenced cells that are within the study area by summing up all yield values within that cells. If yield data points are at the boundary of two adjacent cells, the weight is distributed equally between the cells.

Spatial statistics are quantified using the Cambardella index (CI) [26] and the Mean Correlation Distance (MCD) [27] using variogram parameters extracted from VESPER software [25]. The utility of such studies has been demonstrated in the past [28]. Using an exponential variogram model, the nugget (C_0) and sill ($C_0 + C$) of the yield data are calculated across data points spaced up to 100 m.

The CI is defined as [26]

$$\mathrm{CI} = \frac{C_0}{(C_0 + C)} * 100 \tag{3}$$

and quantifies the extent across which correlation is preserved. A CI value below 25 means strong spatial dependence, CI between 25 and 75 means a moderate spatial dependence, and CI above 75 means a weak spatial dependence.

MCD represents the distance along which correlation is preserved. The MCV is defined as [27]

$$\mathrm{MCD} = \frac{3}{8}\left(\frac{C}{C + C_0}\right)a \tag{4}$$

where a is the range for the variogram or the distance above which value no correlation is detected. The three variogram parameters are estimated for the 2012–2014 yield data acquired across the whole variable rate irrigation area, as well as yield increasing and water efficiency sections. For comparison, the same calculations are carried out for the reference area where year to year variations are small.

III. Results

Differential irrigation is implemented for each irrigation control cell. As an example, in 2013 the yield maximizing section had an overall lower NDVI value compared with the water efficiency section (consistent with the 2012 yield data). Irrigating only the yield maximizing section for the first five weeks (irrigation started on April 28, 2013) the NDVI quickly increased above the water efficiency area's NDVI value. Once the NDVI reverses the trends it can be maintained across the whole growing season by providing more water to the yield maximizing zone. After the first five weeks, all irrigation control cells are irrigated based on the corresponding NDVI values acquired across the growing season. In 2014, the yield maximizing section were irrigated the first four weeks and then all cells were irrigated based on their corresponding NDVI value.

The yield data for each individual irrigation control cell is shown in Fig. 5. The key results of the experiment are summarized in Table I, with the mean values and the coefficient of variation (CoV) (relative standard deviation) for each section and year. The mean yields in the reference and trial areas are similar, at 20.0 and 20.1 tonnes hectare^{-1} for 2012 when the entire vineyard is uniformly irrigated. Lower fruitfulness in 2013 resulted in lower yields compared to 2012. There is no significant improvement in yield in the trial area in 2013, i.e., the yield maximizing and water efficiency sections, which is expected given the growth cycle of grapes. However, a substantial improvement in water efficiency is observed in 2014:

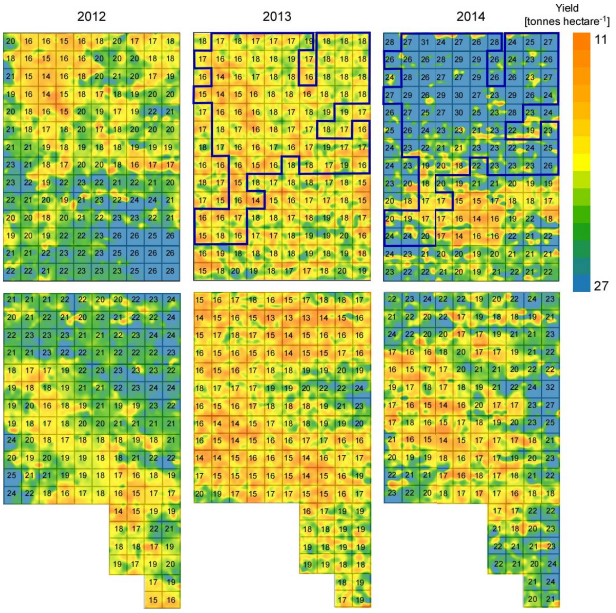

Fig. 5. Top: Yield data for a uniformly irrigated test area in 2012 and a variable rate irrigated test area in 2013 and 2014. For 2013 and 2014, the yield maximizing section is outlined on the top images. Bottom: The yield for the control adjacent area.

TABLE I
YIELD, IRRIGATION WATER, AND WATER EFFICIENCY ANALYSIS FOR THE YIELD MAXIMIZING, WATER EFFICIENCY, AND REFERENCE SECTION OF THE VINEYARD

			2012		2013		2014	
Yield [tonnes hectare^{-1}]			Mean	CoV[%]	Mean	CoV[%]	Mean	CoV[%]
	Trial	Entire area	20.0	14.3	17.2	7.0	22.7	16.7
		Yield section	17.9	9.3	17.0	6.9	24.6	13.1
		Water section	22.5	8.3	17.5	6.7	20.5	15.1
	Reference	Entire area	20.1	11.5	16.8	11.9	19.5	14.6
Irrigation[m^3]	Trial	Entire area			101.0	12.9	99.8	20.4
		Yield section			105.5	12.0	111.8	14.9
		Water section			94.0	11.2	84.1	13.6
	Reference	Entire area			111.0		90.4	
Water efficiency[kg m^{-3}]	Trial	Entire area			5.02	14.5	6.68	14.7
		Yield section			4.68	12.3	6.38	13.5
		Water section			5.4	12.8	7.03	14.3
	Reference	Entire area			4.44	12.3	6.32	18.5

22% for the water efficiency section and 5% for the yield maximizing section. In 2014, yield increased 26% and 5% in the yield and water maximizing sections, respectively. Also, water use efficiency increased by 10% for the water efficiency section, with the water efficiency for the yield maximizing section remaining the same as the reference section.

The CoV for 2013 (Table I) decreased significantly indicating that uniformity of yield distribution is improved more than 50% after the first year (as change in CoV coefficient). After increasing the uniformity, the second year experiment demonstrated that yield trends can be reversed compared to 2012 yield map. In the yield maximizing section where yield is lower in 2012 became high yield areas in 2014 and the high yield area (water efficiency section) in 2012 became low yield in 2014 compared with plot average values. This reversal in yield is possible after only two years using the water as the only parameter that is varied across the trial area. The change in yield trends in 2014 resulted also in an increase of the CoV that is expected considering yield trend reversal.

TABLE II
SPATIAL STATISTICS FOR THE YIELD AND WATER EFFICIENCY SECTION

	Yield	Cambardella Index			Mean Correlation Distance [m]		
		2012	2013	2014	2012	2013	2014
Trial area	Entire area	20.46	23.9	25.38	17.29	2.43	41.74
	Yield section		51.89	33.3		12.54	20.97
	Water section		7.9	34.2		1.9	11.98
Reference area	Entire area	23.6	25.6	24.2	18.53	9.04	13.05

Table II summarizes the CI and MCD values across the three years of yield data. The CI indicates that there is a strong spatial dependence of yield across the variable rate irrigated area and the correlation is preserved for all three years even if the yield has significant spatial changes. The same conclusion is also supported by the MCD that shows a long range correlation with a significant increased value in 2014. Both the Cambardella and MCD values remain very similar for the reference area across the three years of this paper. Variable rate irrigation can change the spatial coherence of yield data on the small scale.

The two-year study on yield and water use efficiency raises two questions. First, why are the yield enhancements small in the first year and significantly larger in the second year? The answer is that grape vines undergo an 18 months growing cycle between bud initiation and harvest [29]. Inflorescence induction and differentiation occurring 18 months prior to harvest are the key factors that govern grape yield potential. Thus, temperature and sunshine as well as stress conditions 18 months prior greatly affect the number of clusters per vine as well as the number of berries per cluster and thus yield [30]. Proper irrigation during bud formation minimizes water stress and its impact is expected to appear at harvest of the second year; which indeed resulted in a 26% increase in the yield in our experiment. The yield increase of 2% in the first year can be attributed to larger berry sizes. The second question is why the water efficiency dropped in the second year from 22% to 10%. Due to water availability constraints in the second year, the start of the irrigation in the reference area is delayed by one month compared to the trial area.

IV. ECONOMIC ANALYSIS

Adoption of the variable rate irrigation technology required new irrigation infrastructure and irrigation analytics calculation.

The first aspect is the change of existing uniform drip irrigation system with a variable rate irrigation system. The practicality of adopting the variable rate technology is influenced by two factors: 1) investment cost and 2) the time for return on investment (ROI). With regards to ROI, the variable rate drip line system is best suited for high variability areas where differential management can improve low

yield cells while managing water efficiently. The cost of a variable rate drip line irrigation system as presented herein depends on the spatial extent of the irrigation control cells. The smaller the control cells, the higher the infrastructure costs will be. Clearly, the size of the irrigation control cell should address yield or soil variability and this will drive the number of control nodes, solenoid valves, etc. Current estimates for implementing the variable rate drip line system at 30 m resolution can approach approximately a one-time cost of $5000 per hectare (assuming large scale fabrication of the components). If the system is fully packaged, installation costs should be similar to today's system. In Fig. 6, the expected yield improvements are calculated as a function of control cell size (i.e., for the yield variability of the vineyard as shown in Fig. 5). Two assumptions are made in this calculation: 1) in regions with lower than average yield, the yield can be increased to the average yield of the field using variable rate irrigation and 2) the maximum yield improvement for the entire field (in the limit of very small control cell sizes) is 20%. We note that 20% is a realistic but potentially conservative assumption given that we have already shown 26% yield improvements. Fig. 6(a) shows that for very small control cells, the benefit of the technology saturates (approaching the assumed 20% maximum yield improvement). For very large control cells, variable rate irrigation becomes ineffective compared to uniform irrigation, which shows that the spatial resolution of the management zone is just too coarse to successfully mitigate the variability. In terms of the cost benefits, an average price of $500 per ton of grapes is assumed, with a potential $1200 profit per acre due to 20% increase in yield. The profit obtained should cover the cost of required new equipment (conversion of single drip line to a double drip line system) and the cost of required electronic components.

Estimates of the ROI at larger manufacturing volumes as a function of the control zone size are shown in Fig. 6(b) with an optimum control cell size of around 30 m × 30 m where the ROI is approximately two years for grapes. Table III quantifies the cost of control electronics as a function of the number of fabricated units where larger volume decreases the unit price for the control nodes. Cost analysis for four distinctive crops indicates the number of years required to recover the investment (Table III-B). We note that all the calculations are made for crops that command high market prices. The ROI for deploying such a variable rate drip line system for strawberries, tomatoes, almonds, and grapes is 0.5, 0.8, 1.6, and 2.5 years, respectively, where the control zone is set at 30 m (the spatial resolution of Landsat imagery). These calculations may change if private satellite imagery needs to be purchased or if the deployed infrastructure will not remain in place for at least five years. Adoption of variable rate irrigation technology can have significant impact in regions such as the Indian subcontinent, most of Africa, Australia, and Western USA where water extraction often exceeds groundwater recharging rates [31].

The second important aspect that needs to be implemented to scale-up variable rate irrigation is the data analytics platform that can ingest large scale geospatial data [32] and

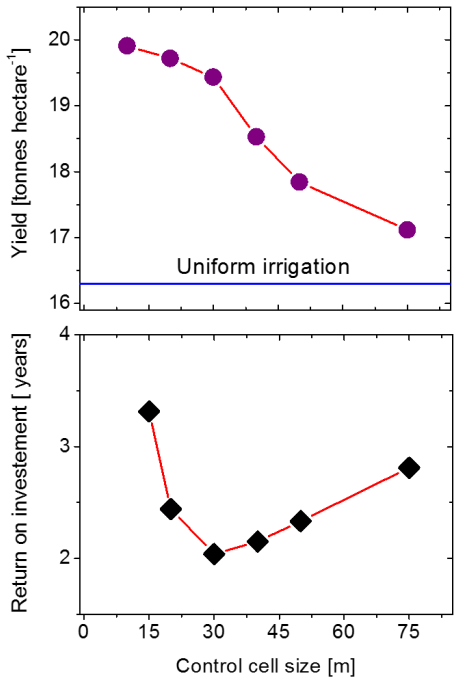

Fig. 6. Expected yield increase and ROI as a function of the control cell's size. The optimum cell size is ∼30 m where the maximum benefits are expected.

create real-time irrigation requirement. Such platforms should automatically combine real-time weather with remotely sensed data and automate and parallelize the analytics that determine the irrigation requirement. Only considered for the continental U.S., the required data sets can be several Terabytes of data each week. Near real-time irrigation prescriptions are virtually impossible using conventional (sequential) data processing techniques due to computational constraints. By way of comparison, a "big" data platform such as a highly distributed file system and processing environment leveraging the MapReduce framework [33] splits these large data files into small manageable 64 kB units, which can then be processed in parallel, thereby enabling computation "in the" data. For example, to scale the irrigation forecasting solution on a global scale we are using more than 32 servers, each with its own multicore processing unit and several local hard discs, where the irrigation analytics can be readily accelerated by a factor of 600 or more. With this system, irrigation requirements can be calculated in near real-time and scaled world-wide and adjusted for unexpected events like excessive precipitation, abrupt changes in daily temperature, and air moisture levels. Current development in big data technology can enable large scale irrigation forecasting using geospatial data [34]. The incremental cost to analyze new satellite data or weather data, in a big data framework, is minimal compared with manual analysis where data download, spatial alignment of data, and running analytics require significant manpower. Automation and machine to machine communication, as demonstrated in this paper, facilitate variable rate irrigation and provide consistency across growing season.

TABLE III
(a) ECONOMIC ANALYSIS OF VARIABLE RATE TECHNOLOGY COST AS FUNCTION OF NUMBER OF CONTROLLED UNITS FABRICATED.
(b) RETURN OF INVESTMENT FOR DIFFERENT CROPS AS FUNCTION OF NUMBER OF CONTROL UNITS USED FOR VARIABLE RATE IRRIGATION

	Number of Control Units		
	1k	100k	1000k
Control box and solenoid valve (per node) ($)	90	70	55
Infrastructure and communication (per hectare) ($)	1450	1235	1000
Assembly (per hectare) ($)	500	430	370
Total cost (per hectare) ($)	8840	7025	5580

(a)

Number of Control Units	Cost of variable rate irrigation/hectare	Return on Investment [years]			
		Strawberry	Almond	Grape	Sugarcane
1k	8.84 k$	0.81	1.92	3.6	20.43
100k	7.02 k$	0.56	1.33	2.5	16.2
1000k	5.58 k$	0.43	1.01	1.9	12.9

(b)

V. DISCUSSION

The above results highlight the benefit of the closed loop variable rate irrigation approach where irrigation is fully automated.

The variable rate drip line system presented here has the advantage of being flexible to deliver water differentially across a spatial area with high temporal resolution. For example, multiple irrigation periods during each day (to maintain constant soil moisture and avoid water pooling) can be readily implemented to maintain constant soil moisture or minimize water usage by applying the right amount of water at the right time.

With proper management zone selection, yield can be significantly improved or water can be saved. The yield maximizing area responded directly to the targeted irrigation and it can be safely assumed that this is the main reason for the improved yield values. The improvements in water efficiency between 10%–20%, demonstrate that similar yields can be obtained using significantly less water. This can be a substantial benefit if the technology is adopted across a large geographical region. If applied to all grape producing region in California, which used 2 billion m^3 irrigation water in 2010 (DWR 2014, USDA 2010), 15% improvements amounts to 300 million m^3 reduction in water usage.

VI. CONCLUSION

This paper validates that: 1) variability can be minimized across a vineyard and 2) low yield areas can be turned into high yield areas using only differential irrigation. Two different objectives, increased yield and preserved water, can be achieved simultaneously in a vineyard by controlling water delivery on a spatial checkboard pattern. We demonstrated that management zone delineation can be defined based on NDVI and yield data and those management zones are a good representation of the variability. This paper demonstrates that with real-time control on the irrigation, the vigor of the canopy can be improved in a few weeks at the beginning of the season and reverse yield patterns after only 2 years of variable rate irrigation. These changes can be achieved on irrigation control cells as low as 15 m $\times$ 15m.

The double drip line system developed for this paper can be easily reconfigured to adjust to any management zones that may affect variability in the field. In locations where soil and management practices vary across the vineyard, dynamic management zones can be defined by clustering the irrigation control cell to reflect the new management zones. Management zone boundaries can be changed dynamically during the growing season by just logically clustering irrigation control cells differently, without changing physical infrastructure.

This proof of concept experiment carried out in a vineyard demonstrates the advantage to automate and customize irrigation for control zones of as little as 40 vines that can result in a 26% improvement in yield and an average 16% increase in water use efficiency. Large scale deployment of variable rate irrigation driven by digital data can enable efficient water use in regions where water is scarce and expensive, as well as during drought, while maintaining and improving currently achievable crop yields.

REFERENCES

[1] Y. Yoo, R. J. Boland, K. Lyytinen, and A. Majchrzak, "Organizing for innovation in the digitized world," *Org. Sci.*, vol. 23, no. 5, pp. 1398–1408, 2012.
[2] A. McBratney, B. Whelan, T. Ancev, and J. Bouma, "Future directions of precision agriculture," *Precis. Agricult.*, vol. 6, no. 1, pp. 7–23, 2005.
[3] L. G. Santesteban, S. Guillaume, J. B. Royo, and B. Tisseyre, "Are precision agriculture tools and methods relevant at the whole-vineyard scale?" *Precis. Agricult.*, vol. 14, no. 1, pp. 2–17, 2013.
[4] R. G. V. Bramley and R. P. Hamilton, "Understanding variability in winegrape production systems," *Aust. J. Grape Wine Res.*, vol. 10, no. 1, pp. 32–45, 2004.
[5] M. Pedroso, J. Taylor, B. Tisseyre, B. Charnomordic, and S. Guillaume, "A segmentation algorithm for the delineation of agricultural management zones," *Comput. Electron. Agricult.*, vol. 70, no. 1, pp. 199–208, 2010.
[6] R. L. Wample, L. Mills, and J. R. Davenport, "Use of precision farming practices in grape production," in *Proc. Precis. Agricult.*, 1999, pp. 897–905.
[7] R. G. V. Bramley and A. P. B. Proffitt, "Managing variability in viticultural production," *Aust. Grapegrower Winemaker*, vol. 427, pp. 11–16, Jul. 1999.
[8] D. L. Corwin and S. M. Lesch, "Apparent soil electrical conductivity measurements in agriculture," *Comput. Electron. Agricult.*, vol. 46, nos. 1–3, pp. 11–43, 2005.
[9] A. Hall, D. W. Lamb, B. P. Holzapfel, and J. P. Louis, "Within-season temporal variation in correlations between vineyard canopy and winegrape composition and yield," *Precis. Agricult.*, vol. 12, no. 1, pp. 103–117, 2011.
[10] A. Tagarakis, V. Liakos, S. Fountas, S. Koundouras, and T. A. Gemtos, "Management zones delineation using fuzzy clustering techniques in grapevines," *Precis. Agricult.*, vol. 14, no. 1, pp. 18–39, 2013.
[11] J. Burrell, T. Brooke, and R. Beckwith, "Vineyard computing: Sensor networks in agricultural production," *IEEE Pervasive Comput.*, vol. 3, no. 1, pp. 38–45, Jan./Mar. 2004.

[12] L. Ruiz-Garcia, L. Lunadei, P. Barreiro, and I. Robla, "A review of wireless sensor technologies and applications in agriculture and food industry: State of the art and current trends," *Sensors*, vol. 9, no. 6, pp. 4728–4750, 2009.
[13] E. J. Knight and G. Kvaran, "Landsat-8 operational land imager design, characterization and performance," *Remote Sens.*, vol. 6, no. 11, pp. 10286–10305, 2014.
[14] D. P. Roy *et al.*, "Landsat-8: Science and product vision for terrestrial global change research," *Remote Sens. Environ.*, vol. 145, pp. 154–172, Apr. 2014.
[15] L. F. Johnson, D. E. Roczen, S. K. Youkhana, R. R. Nemani, and D. F. Bosch, "Mapping vineyard leaf area with multispectral satellite imagery," *Comput. Electron. Agricult.*, vol. 38, no. 1, pp. 33–44, 2003.
[16] L. F. Johnson and T. J. Trout, "Satellite NDVI assisted monitoring of vegetable crop evapotranspiration in California's San Joaquin Valley," *Remote Sens.*, vol. 4, no. 2, pp. 439–455, 2012.
[17] P. S. Chavez, "Image-based atmospheric corrections—Revisited and improved," *Photogramm. Eng. Remote sens.*, vol. 62, no. 9, pp. 1025–1035, 1996.
[18] J. Cai, Y. Liu, T. Lei, and L. S. Pereira, "Estimating reference evapotranspiration with the FAO Penman–Monteith equation using daily weather forecast messages," *Agricult. Forest Meteorol.*, vol. 145, nos. 1–2, pp. 22–35, 2007.
[19] Q. J. Hart *et al.*, "Daily reference evapotranspiration for California using satellite imagery and weather station measurement interpolation," *Civil Eng. Environ. Syst.*, vol. 26, no. 1, pp. 19–33, 2009.
[20] R. G. Allen, L. S. Pereira, D. Raes, and M. Smith, "Crop evapotranspiration-guidelines for computing crop water requirements-FAO irrigation and drainage paper 56," *FAO*, vol. 300, no. 9, 1998, Art. no. D05109.
[21] W. G. M. Bastiaanssen, M. Menenti, R. A. Feddes, and A. A. M. Holtslag, "A remote sensing surface energy balance algorithm for land (SEBAL). 1. Formulation," *J. Hydrol.*, vols. 212–213, pp. 198–212, Dec. 1998.
[22] R. G. Allen, M. Tasumi, and R. Trezza, "Satellite-based energy balance for mapping evapotranspiration with internalized calibration (METRIC)—Model," *J. Irrig. Drain. Eng.*, vol. 133, no. 4, pp. 380–394, 2007.
[23] R. Bramley and S. Williams, *A Protocol for the Construction of Yield Maps From Data Collected Using Commercially Available Grape Yield Monitors*. Glen Osmond, SA, Australia: Cooperat. Res. Centre Viticulture, 2001.
[24] M. J. Pringle, A. B. McBratney, B. M. Whelan, and J. A. Taylor, "A preliminary approach to assessing the opportunity for site-specific crop management in a field, using yield monitor data," *Agricult. Syst.*, vol. 76, no. 1, pp. 273–292, 2003.
[25] B. Minasny, A. B. McBratney, and B. M. Whelan, *VESPER Version 1.62. Australian Centre for Precis. Agriculture*, Univ. Sydney, Sydney, NSW, Australia, 2006.
[26] C. A. Cambardella and D. L. Karlen, "Spatial analysis of soil fertility parameters," *Precis. Agricult.*, vol. 1, no. 1, pp. 5–14, 1999.
[27] S. Han, R. G. Evans, S. M. Schneider, and S. L. Rawlins, "Spatial variability of soil properties on two center-pivot irrigated fields," in *Proc. Precis. Agricult.*, 1996, pp. 97–106.
[28] J. Arnó *et al.*, "Obtaining grape yield maps and analysis of within-field variability in Raimat (Spain)," in *Proc. Precis. Agricult.*, vol. 5, 2005, pp. 899–906.
[29] P. May, *Forecasting the Grape Crop*. Rahuri, India: MPKV, 1972.
[30] L. Sanchez *et al.*, "Effect of a variable rate irrigation strategy on the variability of crop production in wine grapes in California," in *Proc. 12th Int. Conf. Precis. Agricult.*, Sacramento, CA, USA, 2014, pp. 1882–1898.
[31] A. A. Borsa, D. C. Agnew, and D. R. Cayan, "Ongoing drought-induced uplift in the Western United States," *Science*, vol. 345, no. 6204, pp. 1587–1590, 2014.
[32] J. Manyika *et al.*, *Big Data: The Next Frontier for Innovation, Competition, and Productivity*. Washington, DC, USA: McKinsey Glob. Inst., 2011.
[33] A. Aji *et al.*, "Hadoop-GIS: A high performance spatial data warehousing system over mapreduce," *Proc. VLDB Endowment*, vol. 6, no. 11, pp. 1009–1020, 2013.
[34] L. J. Klein *et al.*, "PAIRS: A scalable GEO-spatial data analytics platform," in *Proc. IEEE Int. Conf. Big Data (Big Data)*, Santa Clara, CA, USA, 2015, pp. 1290–1298.

Levente J. Klein received the Ph.D. degree in physics from the University of Utah, Salt Lake City, UT, USA.

Since 2006, he has been with the IBM T. J. Watson Research Center, Yorktown Heights, NY, USA, where he developed technologies to enable energy efficient cooling in data centers, monitoring fugitive methane gas in oil and gas industry, and application of wireless sensing solution in agriculture and healthcare, and has been a Research Staff Member with the Internet of Things and Industry Solution. His research with the IBM T. J. Watson Research Center spans multidisciplinary research topics from material science, nano-optics, and wireless sensing solutions with strong focus to apply research technologies to industrial problems.

Dr. Klein was a recipient of three of IBM's Outstanding Technical Achievement Awards and multiple IBM Research Division Awards for his research.

Hendrik F. Hamann (M'01) received the Ph.D. degree from the University of Göttingen, Göttingen, Germany.

In 1999, he joined the IBM T. J. Watson Research Center, Yorktown Heights, NY, USA, where he is leading the Physical Analytics and Cognitive Internet of Things Program and is currently a Senior Manager and a Distinguished Research Staff Member. He is an IBM Master Inventor, a member of the IBM Academy of Technology, Armonk, NY, USA, and has served on governmental committees such as the National Academy of Sciences and the National Science Foundation, and as an Industrial Advisor to universities. He has authored or co-authored over 120 peer-reviewed scientific papers and holds over 120 patents and has over 130 pending patent applications. His current research interests include sensor networks, sensor-based physical modeling, machine-learning, and artificial intelligence, as well as big data technologies.

Dr. Hamann was a recipient of several awards, including the 2016 AIP Prize for Industrial Applications of Physics. He is a member of the American Physical Society, Optical Society of America, and the New York Academy of Sciences.

Nigel Hinds received the M.S. and Ph.D. degrees in computer science from the University of Michigan, Ann Arbor, MI, USA.

He is a Technical Staff Member with the IBM Research Division, IBM T. J. Watson Research Center, Yorktown Heights, NY, USA. He has contributed to the NASA Earth Observing System project, as well as Linux open source. He has developed power saving communication protocols for wireless networks. His current research interests include operating systems, distributed resource management, and large scale data analytics systems.

Supratik Guha received the B.Tech. degree from the Indian Institute of Technology Kharagpur, Kharagpur, India, in 1985, and the Ph.D. degree in materials science from the University of Southern California, Los Angeles, CA, USA, in 1991.

He was the Director of Physical Sciences with the IBM T. J. Watson Research Center, Yorktown Heights, NY, USA. He joined Argonne National Laboratory, Lemont, IL, USA, in 2015, where he is currently the Division Director of the Center for Nanoscale Materials. In 2015, he also joined the University of Chicago, Chicago, IL, USA, where he is currently a Professor with the Institute for Molecular Engineering.

Luis Sanchez is a Researcher with the Ernest & Julio Gallo Winery, Modesto, CA, USA.

Brent Sams is a Researcher with the Ernest & Julio Gallo Winery, Modesto, CA, USA.

Nick Dokoozlian is a Researcher with the Ernest & Julio Gallo Winery, Modesto, CA, USA.